

1  
2  
3  
4  
5  
6  
7  
8  
9  
10  
11  
12  
13  
14  
15  
16  
17  
18  
19  
20  
21  
22  
23

**Advancing age grading techniques for *Glossina morsitans*  
*morsitans*, vectors of African trypanosomiasis, through mid-  
infrared spectroscopy and machine learning**

Mauro Pazmiño-Betancourth<sup>1</sup>, Ivan Casas Gómez-Uribarri<sup>1</sup>, Karina Mondragon-Shem<sup>2</sup>,  
Simon A Babayan<sup>1</sup>, Francesco Baldini<sup>1,3\*, §</sup>, Lee Rafuse Haines<sup>2,4\*, §</sup>

<sup>1</sup>School of Biodiversity, One Health and Veterinary Medicine, University of Glasgow, UK, G12 8QQ

<sup>2</sup>Department of Vector Biology, Liverpool School of Tropical Medicine, UK, L3 5QA

<sup>3</sup>Ifakara Health Institute, Environmental Health, and Ecological Sciences Department, Morogoro, United  
Republic of Tanzania

<sup>4</sup>Department of Biological Sciences, University of Notre Dame, USA, 46556

[\\*Francesco.Baldini@glasgow.ac.uk](mailto:Francesco.Baldini@glasgow.ac.uk), [lhaines@nd.edu](mailto:lhaines@nd.edu)

<sup>§</sup>These authors equally supervised the work

**Corresponding authors:**

[Francesco.Baldini@glasgow.ac.uk](mailto:Francesco.Baldini@glasgow.ac.uk), [lhaines@nd.edu](mailto:lhaines@nd.edu)

**Short title (70 characters):**

Mid-infrared spectroscopy and machine learning for tsetse surveillance

## 24 **Abstract**

25 Tsetse are the insects responsible for transmitting African trypanosomes, which cause  
26 sleeping sickness in humans and animal trypanosomiasis in wildlife and livestock. Knowing  
27 the age of these flies is important when assessing the effectiveness of vector control programs  
28 and modelling disease risk. However, current methods to assess fly age are labour-intensive,  
29 slow, and often inaccurate as skilled personnel are in short supply. Mid-infrared spectroscopy  
30 (MIRS), a fast and cost-effective tool to accurately estimate several biological traits of insects,  
31 offers a promising alternative. This is achieved by characterising the biochemical composition  
32 of the insect cuticle using infrared light coupled with machine learning algorithms to estimate  
33 the traits of interest.

34 We tested the performance of MIRS in estimating tsetse sex and age for the first time using  
35 spectra obtained from their cuticle. We used 541 insectary-reared *Glossina m. morsitans* of  
36 two different age groups for males (5 and 7 weeks) and three age groups for females (3 days,  
37 5 weeks, and 7 weeks). Spectra were collected from the head, thorax, and abdomen of each  
38 sample. Machine learning models differentiated between male and female flies with a 96%  
39 accuracy and predicted the age group with 94% and 87% accuracy for males and females,  
40 respectively. The key infrared regions important for discriminating sex and age classification  
41 were characteristic of lipid and protein content. Our results support the use of MIRS as a fast  
42 and accurate way to identify tsetse sex and age with minimal pre-processing. Further  
43 validation using wild-caught tsetse can pave the way for this technique to be implemented as  
44 a routine surveillance tool in vector control programmes.

45

46

47 **Author summary (150-200)**

48 Male and female tsetse transmit the parasites that cause sleeping sickness in humans and  
49 nagana in livestock. To control these diseases, knowing the age of these flies is important, as  
50 it helps evaluate the efficacy of control measures and assess disease risk. However, current  
51 age-grading methods are laborious, often unreliable, and in the case of male tsetse, highly  
52 inaccurate. This study explores a novel approach that uses mid-infrared spectroscopy (MIRS)  
53 to estimate the age of individual tsetse. Machine learning can detect signatures in MIRS that  
54 help identify the composition of a fly's cuticle, which differs between sexes and changes as  
55 they age.

56 We trained machine learning models that distinguished male from female flies with 96%  
57 accuracy and predicted the correct age group with 94% accuracy for males and 87% accuracy  
58 for females. MIRS offers a fast and reliable way to identify tsetse sex and age with minimal  
59 preparation. If this method is successfully validated with wild flies, it holds the potential to  
60 vastly increase the accuracy of the way we monitor and combat these disease-carrying  
61 insects, thus offering significant advantages in our efforts to control them.

62

63

64

65

66

## 67 **Introduction**

68 Tsetse are blood-feeding flies that can transmit trypanosome parasites of human and animal  
69 concern. There are two parasite species that cause Human African Trypanosomiasis (HAT), or  
70 sleeping sickness, and infected patients can die if they do not receive treatment. The  
71 promising decline of cases in endemic areas[1] in recent years is due to ongoing disease and  
72 vector control efforts, but continued support is critical to ensure the success of disease  
73 elimination programmes. However, Rhodesiense HAT (the more severe form) is still a concern  
74 due to livestock and wildlife forming part of its transmission cycle. Animal African  
75 trypanosomiasis (AAT) affects wildlife and domestic animals, causing three million cattle  
76 deaths/year with agricultural losses nearing US\$ 5 billion/year[2]. Both female and male  
77 tsetse can transmit trypanosomes, but only adult flies older than 20 days post-emergence  
78 that have ingested blood from a parasite-infected host can be infectious. Tsetse age is  
79 therefore crucial for estimating transmission risk and the efficacy of vector control  
80 programmes. Accurate age grading in the field is crucial for disease monitoring and evaluation  
81 operations. An effective vector control intervention, which does not discriminate against age,  
82 overall will reduce the average age of tsetse populations. For example, if in an area of ongoing  
83 vector control only young flies are caught, this suggests newly emerged flies in the area,  
84 whereas capturing older flies either indicates fly reinvasion from outside the intervention  
85 zone or intervention failure.

86 Tsetse age grading for female flies currently relies on performing a labour-intensive ovarian  
87 dissection, which requires the use of a microscope and an experienced dissector. Female  
88 tsetse give birth to a larva every 9 days[3] throughout life, and the four ovarioles develop in  
89 a specific, predictable sequence; as each egg descends into the uterus, it leaves behind a scar

90 (named 'relic') that can be microscopically identified[4]. No new relics are created after the  
91 4th ovarian cycle, thus limiting the confidence of this method in flies older than seven  
92 weeks[4]. Furthermore, factors such as nutritional stress[5] , tsetse strain[6] and  
93 temperature[7] can affect the length of this 9-day process, and even with adjustments, the  
94 method can be imprecise. Ovarian dissections are time consuming and need to be performed  
95 while the tsetse is still 'fresh', and tissues maintain their form. After death, flies quickly  
96 become dehydrated and age grading is no longer possible by this method. This makes it  
97 difficult to process large numbers of flies when monitoring control interventions.

98 The current situation is worse for male tsetse, as there are no dependable methods for age-  
99 grading them. Wing fray analysis in either wild male[8] or female flies is unreliable as artifacts  
100 can be introduced through trapping protocols. Other approaches like tsetse eye pigment  
101 (pteridine) analysis[9] and gene expression [10] are too complex or costly for routine use in  
102 field settings. Thus, all current age-grading methods are either too imprecise, laborious, or  
103 expensive.

104 Mid-infrared spectroscopy (MIRS) has proven to be a versatile technique for determining  
105 mosquito age and species in both insectary-reared and field-collected mosquitoes[11–14].  
106 MIRS quantifies the energy a molecule absorbs based on its molecular vibrations[15,16]. As  
107 the insect surface is covered with a complex mixture of cuticular proteins, polysaccharides,  
108 wax and other lipids, this tool provides a way to detect the differences between different  
109 samples. The chemical composition of male and female cuticles, as well as different species-  
110 specific signatures, can be resolved alongside more transient aspects such as cuticular  
111 changes over time[17]. Scanning a dried insect sample with MIRS is fast (1-2 minutes), and  
112 when combined with the use of machine learning (ML) algorithms, it provides a powerful

113 toolbox for researchers to rapidly assess vector populations with minimum sample processing  
114 and high accuracy.

115 In this study, we use ML to estimate the age and sex from MIRS of different fly tissues  
116 collected from insectary-reared tsetse (*Glossina morsitans morsitans*) of known age and sex.  
117 We also identified the regions of the tsetse mid-infrared spectrum associated with age and  
118 sex, to elucidate the biological basis of our model predictions.

119

## 120 **Methods**

### 121 **Tsetse rearing**

122 An age-stratified colony of *Glossina morsitans morsitans* Westwood, established in 2004 at  
123 the Liverpool School of Tropical Medicine (LSTM), UK, was daily maintained under the  
124 following conditions: 26 – 28 °C, 68 – 78 % humidity and a 12 h/12 h light/dark cycle. Tsetse  
125 were fed three times a week on sterile defibrinated horse blood (TCS Biosciences Ltd,  
126 Buckingham, UK) using a silicon membrane feeding system.

### 127 **Tsetse sampling strategy and desiccation**

128 Young, unmated female flies were first collected from emerging pupal pots as male  
129 emergence is delayed, and male collection was timed after the females had emerged. Both  
130 teneral (unfed, newly emerged) female and male collections were isolated from each other  
131 to prevent potential cuticular contamination with contact sex pheromones (cuticular  
132 hydrocarbon) during mating[18].

133 We collected 354 female and 187 male teneral tsetse from the LSTM colony in total for  
134 analysis. At specific ages, tsetse were killed with chloroform-soaked cotton, placed on a thin  
135 layer of cotton wool inside a 15 ml falcon tube half-filled with silica gel beads, sealed and then  
136 stored at 4°C until required. Desiccated tsetse were transferred to 96-well plates in  
137 preparation for shipping to the University of Glasgow. Upon analysis, dried flies were  
138 dissected into three sections: head, thorax and abdomen using dissection tweezers.

### 139 **Infrared Spectroscopy**

140 Spectra from individual heads, thoraces and abdomens were taken by Attenuated Total  
141 Reflection (ATR) FT-IR spectroscopy using a Bruker ALPHA II spectrometer equipped with a  
142 Globar lamp, a deuterated L-alanine doped triglycene sulphate (DLATGS) detector, a  
143 Potassium Bromide (KBr) beam splitter, and a diamond ATR accessory (Bruker Platinum ATR  
144 Unit A225). Twenty-four scans were collected at room temperature between 4000 and 400  
145  $\text{cm}^{-1}$  with  $4 \text{ cm}^{-1}$  resolution per sample. When measuring the tsetse samples, we made efforts  
146 to avoid practices that introduce sources of bias such as: not always measuring first young  
147 and then old samples, or first females and then males. Low-quality spectra were discarded  
148 using a custom script designed for mosquito spectra [11,19].

### 149 **Machine learning analysis**

150 Spectra were centred around a mean of 0 and scaled to a standard deviation of 1 prior to any  
151 analysis. Uniform Manifold Approximation and Projection (UMAP) was applied for clustering  
152 analysis. Sex and age groups were binarized using one hot encoding[20]. First, we shuffled  
153 and split the dataset into the training (80%) and test sets (20%), stratified by sex and age  
154 groups (Supplementary Material Table S1). The training set was used to compute baseline  
155 performance of four machine learning algorithms: Logistic Regression (LR), Random Forest

156 (RF), Support vector machine (SVC) and Classification and Regression Tree (CART) using 10-  
157 fold cross validation and default parameter settings on the training set. Additionally, a  
158 permutation score test was performed to evaluate if there was a dependency between the  
159 features (absorbance of each wavenumber) and classes (sex and age groups) (Supplementary  
160 Material Fig S1). The best model was then optimized using hyperparameter tuning, which  
161 consists in choosing a set of optimal values for the model hyperparameters to maximize its  
162 performance. The remaining 20% of the data (the test set) was used for the final evaluation  
163 of the optimized models. The individual metrics used to evaluate the models were accuracy,  
164 sensitivity, and specificity. Machine learning was performed using Python 3.10 and scikit-learn  
165 1.2.2.

## 166 **Data and code availability**

167 The infrared spectral data generated for this study have been deposited in the Enlighten  
168 database and are available at <http://dx.doi.org/10.5525/gla.researchdata.1564>.

169 All code to reproduce the machine learning analysis and figures is available at  
170 [https://github.com/maurocolapso/Pazmino\\_TsetseMIRS\\_2023.git](https://github.com/maurocolapso/Pazmino_TsetseMIRS_2023.git)

## 171 **Results**

### 172 **Optimization of tsetse desiccation**

173 To understand how long it took for tsetse in different nutritional states to fully dehydrate  
174 (which is key to avoid the noise in the spectra caused by the water signal), we placed  
175 individual tsetse into 15ml tubes containing a deep layer of silica gel under a thin cap of cotton  
176 wool. Fly weight loss was daily recorded until it stabilised. Unfed flies rapidly desiccated within  
177 24h, while fully engorged, bloodfed male and female flies took over three days to dehydrate



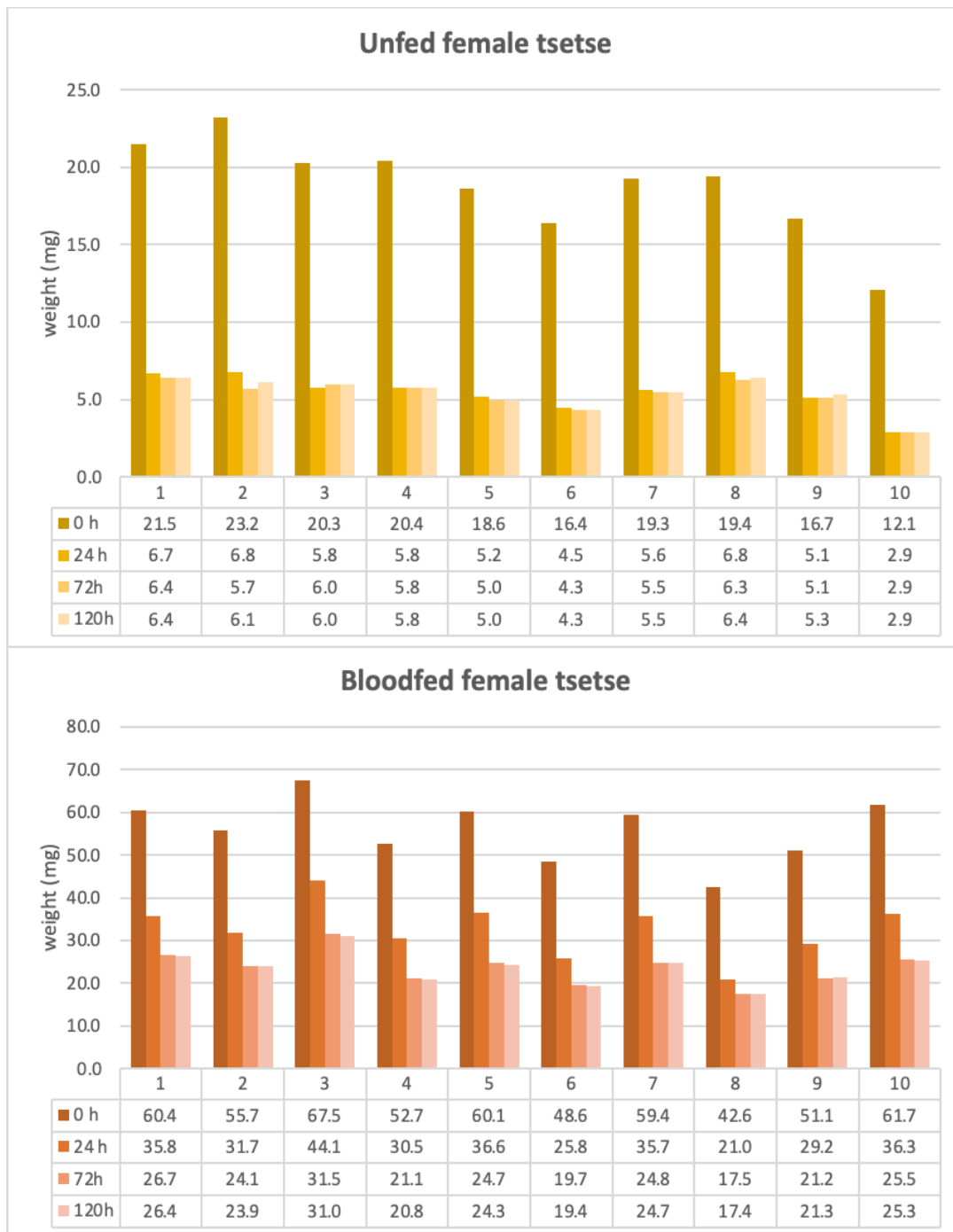
178 the water-rich meal. Based on this data we adopted a standardized ~72h of desiccation on

179 silica for all flies subjected to MIRS analysis (**Error! Reference source not found.**)

180

181

**Table 1.** Desiccation time test for unfed and bloodfed female and male tsetse



182

183

## 184 Differences between tsetse tissues

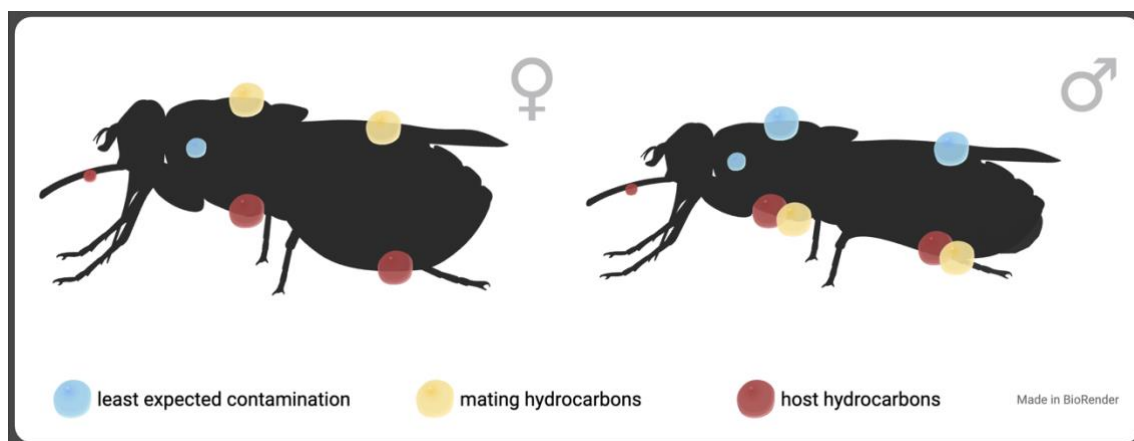
185 Initial tests focused on finding the best body regions or tissues to give a high signal clarity

186 when doing spectrometric readings, as the large size tsetse presented novel logistical

187 challenges. Because wild-caught flies are likely to acquire foreign hydrocarbons from mating,

188 blood feeding, or the resting environment, we sampled zones of the cuticle expected to show  
189 the least contamination (**Error! Reference source not found.**).

190



191

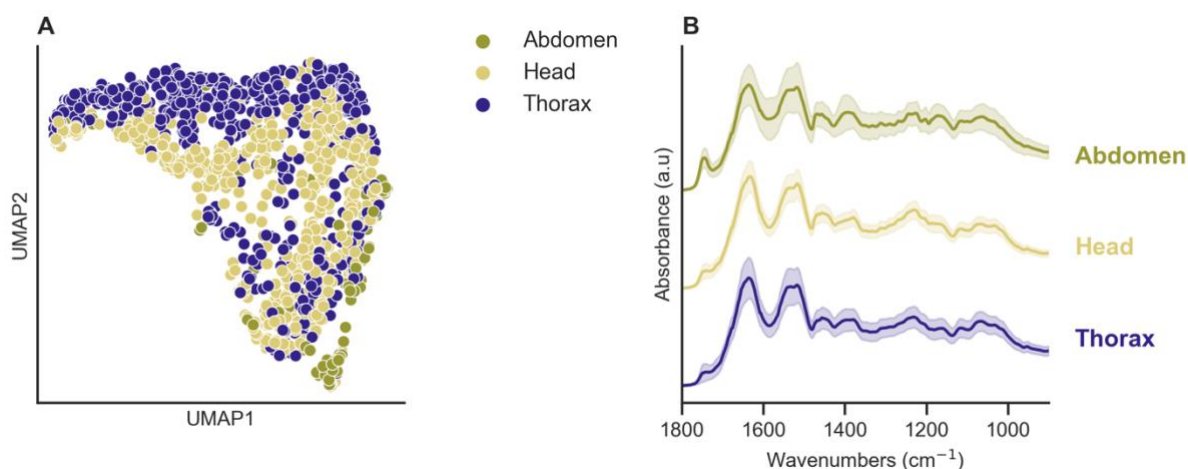
192 **Fig 1.** Tsetse biology and ecology suggest the heads and dorsal side of male tsetse or the  
193 lateral side of the thorax in both sexes would be the best areas (blue circles) to detect  
194 individual cuticular hydrocarbons.

195

196 We further investigated the variation between spectra of different tissues. Spectra from fly  
197 abdomens differed substantially those from heads and thoraces (Fig 2A), showing lower  
198 intensity and a higher variability, especially in the 1800 to 900  $\text{cm}^{-1}$  region (Fig 2B). Moreover,  
199 visual inspection of the abdomens indicated that despite ~60 days in a sealed anhydrous  
200 environment, complete desiccation was not achieved, particularly if the fly had ingested a  
201 large blood volume prior to collection. This residual horse blood and water could be driving  
202 the greater variability of the abdominal spectra compared to the other tissues. On top of that,  
203 previous work in other insects showed the thorax as a target tissue for MIRS. Consequently,  
204 we decided to focus our analysis on the spectra obtained from heads and thoraces only. A  
205 total of 1071 spectra were obtained by scanning the heads and lateral part of the thoraces of  
206 541 flies of different ages (Fig 1, Table 2).

207

208



209

210 **Fig 2. Spectra comparison from the abdomen, head, and thorax.** **A)** Uniform Manifold  
 211 Approximation and Projection (UMAP) of the abdomens, heads, and thoraces showed that  
 212 the spectra collected from abdomens formed a separate cluster. Abdomens (olive green),  
 213 head (yellow), thorax (purple) **B)** High variability of the spectra from abdomens (olive green  
 214 line) showed that the sources of those inconsistencies were of low intensity and great  
 215 variability at some wavelengths (primarily in the 1800 to 900  $\text{cm}^{-1}$  region) compared to spectra  
 216 from head (yellow line) and thorax (purple line). Spectra shown in panel B have been manually  
 217 shifted across the Y-axis for ease of comparison.

218

219

**Table 2.** Summary of aggregated samples sizes.

| Sex                            | Age     | Tissue | # spectra   | # samples  |
|--------------------------------|---------|--------|-------------|------------|
| Female                         | 3 days  | Head   | 133         | 136        |
|                                |         | Thorax | 136         |            |
|                                | 5 weeks | Head   | 92          | 96         |
|                                |         | Thorax | 96          |            |
|                                | 7 weeks | Head   | 120         | 122        |
|                                |         | Thorax | 122         |            |
| Male                           | 5 weeks | Head   | 94          | 94         |
|                                |         | Thorax | 93          |            |
|                                | 7 weeks | Head   | 93          | 93         |
|                                |         | Thorax | 92          |            |
| <b>Total number of samples</b> |         |        | <b>1071</b> | <b>541</b> |

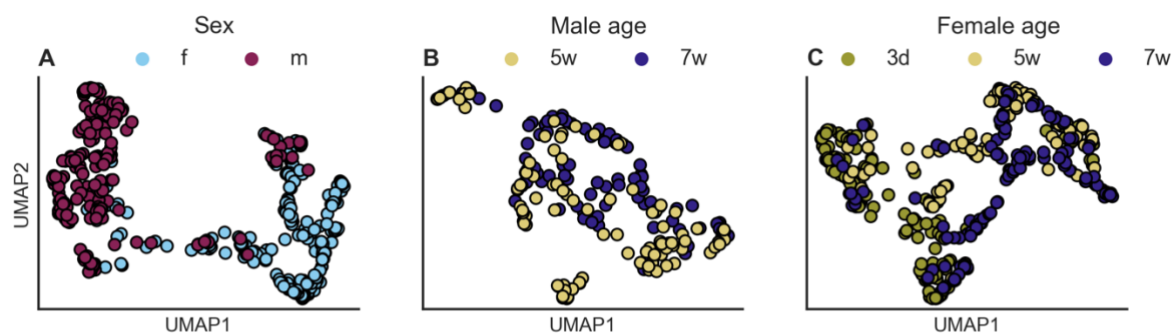
## 220 **Differences between sexes and age groups**

221 We used the unsupervised machine learning algorithm Uniform Manifold Approximation and  
222 Projection (UMAP) to investigate whether the spectra from fly heads (  
223 Fig 3 A-C) and thoraces (  
224 Fig 3 D-F) differed between flies of different sex and age. Most of the male flies produced  
225 different spectra than females, with the thorax showing clearer clusters with fewer samples  
226 overlapping between them (**Fig 3 A and D**). For age groups, there were not clusters in males  
227 regardless the tissue (**Fig 3 B and E**). In females, there were a distinct cluster composed of old  
228 flies (5 and 7 weeks) when using the thorax, however, there was a high overlap between  
229 samples from different age groups (**Fig 3 C and F**). These results show that MIRS contains  
230 biochemical information associated with sex and age as expected from relative changes in the  
231 cuticular composition of tsetse.

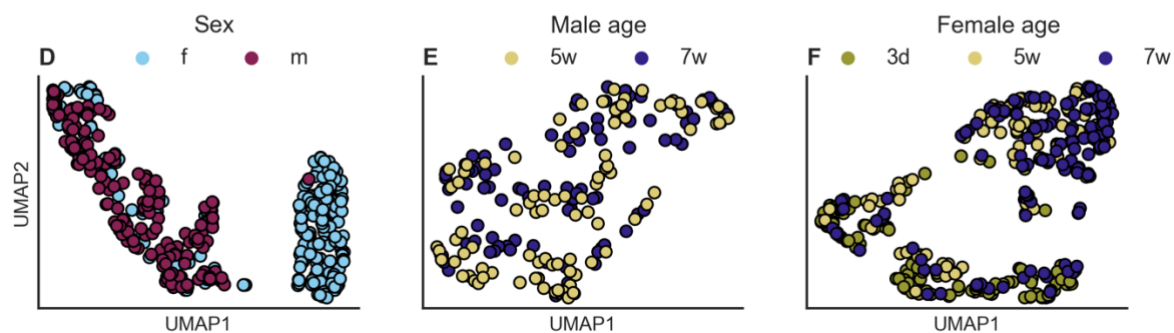
232

233

## Head



## Thorax



234

235 **Fig 3. MIRS spectra according to tsetse sex and age from specific tissues.** Unsupervised  
236 clustering of MIRS measurements using Uniform Manifold Approximation and Projection of  
237 MIRS in two-dimensional space using the heads and thorax. Samples are coloured by: **A, D)**  
238 sex (females: blue, males: purple). **B, E)** Males coloured by age (5 weeks: yellow, 7 weeks:  
239 dark blue). **C, F)** Females coloured by age (3 days: olive green, 5 weeks: yellow, 7 weeks:  
240 dark blue)

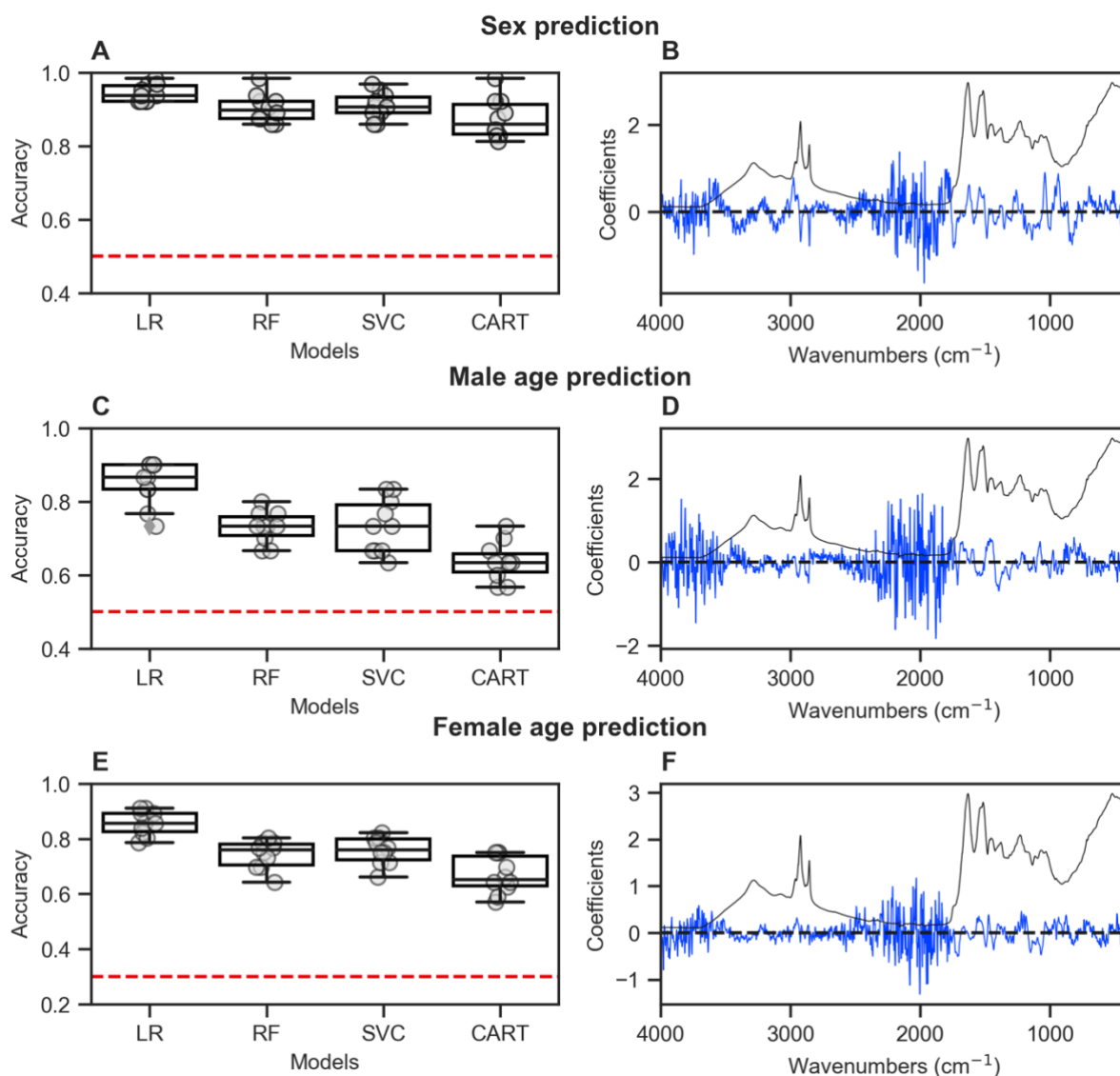
241

## 242 Sex and age prediction using the complete spectral data

243 To identify tsetse sex and age-specific patterns within our MIRS dataset, we compared logistic  
244 regression (LR), Random Forest (RF), support vector machine (SVC) and the Classification and  
245 Regression Tree (CART) algorithms. Among these, LR had the highest accuracy (Fig 4A) when  
246 estimating the sex of five- and seven-week-old flies. Training accuracy was 94% when using  
247 both head (Fig 4A) and thorax (Supplementary Material Table S2). Similar accuracies were  
248 obtained in the test set (head = 99%, thorax = 94%, Supplementary Material Table S2). Logistic  
249 Regression was also the most accurate algorithm for identifying age groups among flies of the

250 same sex (Fig 4C). For males, the thorax was marginally better at age prediction with an  
251 accuracy of 88% compared to 85% for the head (Supplementary Material Table S2). Similar  
252 performance was found in the test set with 92% and 89% for thorax and head, respectively  
253 (Supplementary Material Table S2). In females, even though there was some difference in  
254 accuracy between the head and thorax on the training set (head = 86%, thorax = 92%),  
255 accuracy on the test set was similar for both tissues at 93% (Supplementary Material Table  
256 S2). While these initial results suggest that infrared spectra could be used to predict key  
257 biological traits of tsetse flies, further analysis of model coefficients suggested that the  
258 predictions were being based mostly on flat regions of the spectra, between  $4000 - 3750 \text{ cm}^{-1}$   
259  $^1$  and  $2250 - 1800 \text{ cm}^{-1}$  (Fig 4 B, D and E), which are unlikely to contain biochemical  
260 information associated with insect cuticle[11] and are primarily used to monitor the presence  
261 of  $\text{CO}_2$  in the environment[15]. This phenomenon was observed with all predictive algorithms  
262 regardless of what tissue was used. To further investigate this, we applied the framework by  
263 Eid et al. [21]. Briefly, we divided the spectrum into three parts: two regions known to contain  
264 vibrations from key chemical bonds ( $3500 - 2500 \text{ cm}^{-1}$  and  $1800 - 600 \text{ cm}^{-1}$ ) and one region  
265 where no chemical information associated with insect cuticle is expected ( $2500 - 1800 \text{ cm}^{-1}$ ).  
266 We then compared the accuracy of four algorithms: Logistic regression, SVM with two kernels  
267 (RBF and linear) and Random Forest on each region. While the biochemical fingerprint regions  
268 ( $3500 - 2500 \text{ cm}^{-1}$ ,  $1800 - 600 \text{ cm}^{-1}$ ) gave variable prediction accuracies (60 – 96%), when  
269 using the region with no chemical information associated with insect cuticle ( $2500 - 1800 \text{ cm}^{-1}$ ).  
270  $^1$ ), two algorithms (Logistic Regression and SVM with a linear kernel) could still predict  
271 different traits with high accuracy (83 – 94%), indicating possible overfitting (Supplementary  
272 Table S3). To produce more generalisable models, we therefore chose to base our predictions

273 on the spectral region of 1800 – 600  $\text{cm}^{-1}$ , which is known to contain the most relevant  
274 biochemical information in insects[12–14].



275

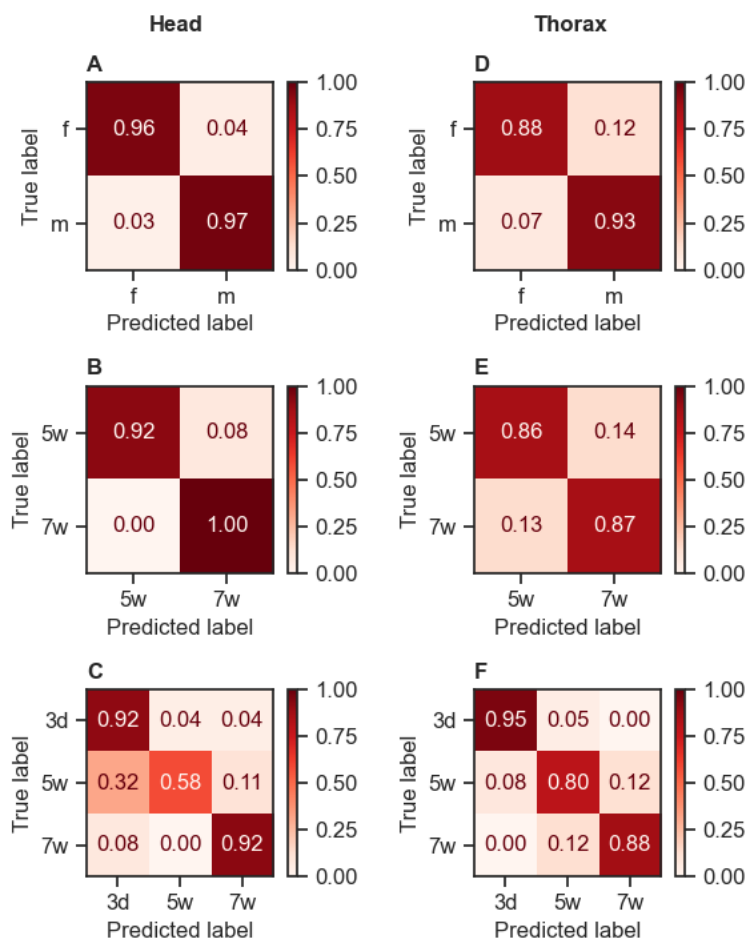
276 **Fig 4. Prediction of tsetse sex and age using MIRS.** Model performance on the training set of  
277 various ML models (LR: Logistic regression, RF: random forest, SVC: support vector machine  
278 and CART: decision tree classifier) for sex and age prediction using the heads of tsetse (**A**, **C**,  
279 **E**). Boxplots show the distribution of accuracies using 10-fold cross-validation. The horizontal  
280 dashed red line indicates a 0.5 accuracy for binary predictions (**A**, **C**) and 0.3 for a three-class  
281 prediction (**E**). Coefficients of the best model (blue line) plotted against the mean spectra of  
282 tsetse (**B**, **D**, **F**) show how the model relies on the 4000 – 3500 and 2500 – 1800  $\text{cm}^{-1}$  regions  
283 for prediction, which are lacking key biological information.

284



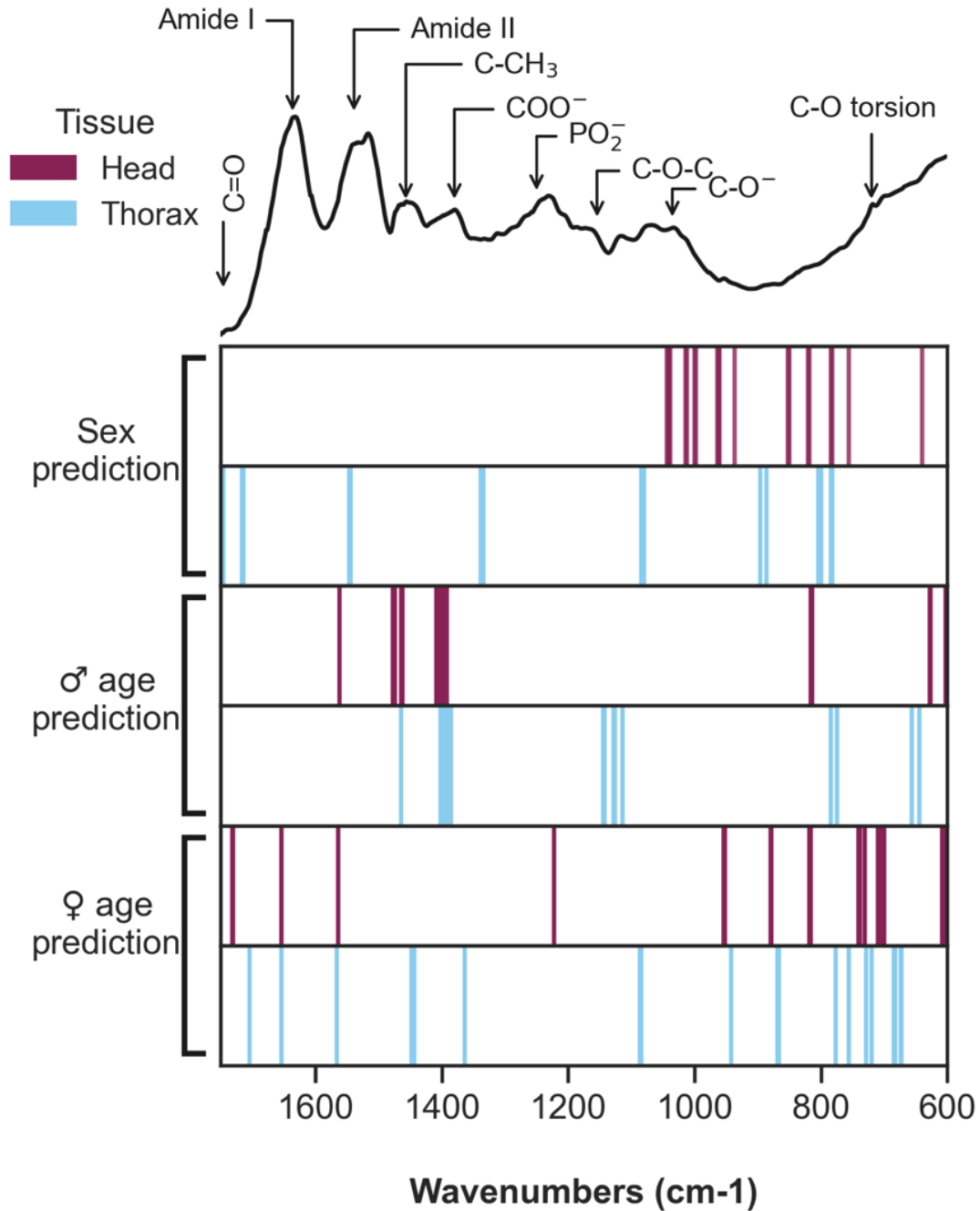
## 285 **Sex and age prediction using the biochemical fingerprint region of** 286 **the spectra**

287 When considering only the spectral region from 1750 - 600  $\text{cm}^{-1}$ , the accuracy of predicting  
288 fly sex and age marginally declined regardless of the algorithm used for analysis  
289 (Supplementary Material Fig S2). Logistic regression was able to clearly predict sex using the  
290 spectra from the heads with an accuracy of 96% (Fig 5A). The most informative wavenumbers  
291 appeared around the 1000 and 800  $\text{cm}^{-1}$  areas of the spectra (Fig 6). Logistic regression was  
292 able to predict 5-week vs. 7-week-old males using spectral data from the head with an  
293 accuracy of 95% (Fig 5B). Most of the coefficients used by this model were in the 1636 and  
294 1400  $\text{cm}^{-1}$  region (Fig 6**Fig 6**). Finally, age prediction in females was better when using the  
295 thorax. Young teneral flies were identified by the model with over 90% accuracy and older  
296 flies with 80% accuracy (Fig 5F). Like males, the important wavenumbers were in the same  
297 range, the 1750 to 1450  $\text{cm}^{-1}$  800 to 600  $\text{cm}^{-1}$  region (Fig 6). However, when using spectral  
298 data from the head, the model struggled to identify the 5-week-old age group; an accuracy of  
299 58% (Fig 5C) was obtained, which was likely influenced by several 5-week-old samples being  
300 misclassified as 3-day-olds. A summary of the performance of Logistic Regression is shown in  
301 Table 3 and wavenumber importance and their assignments are presented in Supplementary  
302 Table S4. These results suggest that MIRS-ML is a promising approach when using the tsetse  
303 head or thorax to reliably produce quality spectra for sex and age prediction of laboratory-  
304 reared flies.



305

306 **Fig 5. Confusion matrix for predicting tsetse sex and age using reduced number of**  
307 **wavenumbers.** Accurate identification of females (f) and males (m) (**A, D**) and two-week age  
308 difference (5 weeks (5w) vs 7 weeks (7w) old) in male flies (**B, E**). Spectra from the thoraces  
309 of young female flies (3d post emergence) compared to older female flies (5 weeks (5w) and  
310 7 weeks (7w) old (**C, F**)



311

312 **Fig 6. Important wavenumbers for predicting tsetse sex and age change depending on the**  
313 **trait predicted.** Coloured lines represent the position of the most informative wavenumbers  
314 used by the models to predict sex, male age, and female age. Lines are coloured depending  
315 on the tissue used for MIRS: head (purple), thorax (light blue). Example spectra with band  
316 assignments is added on the top for reference.

317

318 **Table 3.** Accuracy, sensitivity and specificity of tsetse sex and age prediction on males and  
319 females in the training set and test set

|                                   | <b>Tissue</b> | <b>Accuracy<br/>(train set)</b> | <b>Accuracy<br/>(test set)</b> |
|-----------------------------------|---------------|---------------------------------|--------------------------------|
| <b>Sex prediction</b>             | Head          | 0.95 ± 0.04                     | 0.96                           |
|                                   | Thorax        | 0.93 ± 0.03                     | 0.90                           |
| <b>Males age<br/>prediction</b>   | Head          | 0.85 ± 0.06                     | 0.94                           |
|                                   | Thorax        | 0.82 ± 0.06                     | 0.86                           |
| <b>Females age<br/>prediction</b> | Head          | 0.84 ± 0.05                     | 0.83                           |
|                                   | Thorax        | 0.85 ± 0.04                     | 0.87                           |

320

## 321 **Discussion**

322 Here, we showed for the first time how a MIRS + ML toolbox can be applied to predict the sex  
323 and age of desiccated insectary-reared tsetse. The spectra collected from the head and  
324 thorax, but not the abdomen, allow accurate sex prediction. Age grading was successful in  
325 both sexes, even when flies were only two weeks apart in age. When using exclusively the  
326 thorax, this toolbox can easily differentiate between females and males using the infrared  
327 region related to lipids and carbohydrates. Interestingly, predictions using the head identified  
328 a narrow spectral region related to lipids as the most informative. It has been previously  
329 reported that *G. pallidipes* females possess a higher amount of cuticular lipids than males[22],  
330 which is likely linked to the female sex pheromone that constitutes the main cuticular  
331 hydrocarbon. Considering this potential bias, we did not mix the two sexes for analysis since  
332 the signal difference can mask the differences between the ages of each sex.

333 When analysing the most important regions for age grading in both males and females, some  
334 clear patterns emerged depending on the tissue and biological trait. In male flies, the C-CH<sub>3</sub>

335 and COO<sup>-</sup> bands were consistently important in age grading for all tissues. However, the bands  
336 related to proteins and lipids and the -(CH<sub>2</sub>)-rock functional group related to wax was  
337 important across female tissues. Characterizing the informative and predominant  
338 wavenumbers is an important for understanding the association between age and absorption  
339 bands, which can be used to optimize data collection or model generalisation. An early  
340 staining method showed a relationship between cuticular layers in the thorax from laboratory  
341 and field caught flies[23]. Other methods using gene expression panels have also found that  
342 genes related to cuticular proteins were important for age grading. One study used RNAseq  
343 to analyse gene expression associated with age and sex in *G. m. morsitans* that were sourced  
344 from the same colony at LSTM [7]. Out of the ten genes shortlisted in the study, two proved  
345 to be enough for accurate age classification, one of these being cuticular protein 92F  
346 (GMOY002920). A second cuticular protein, 49Aa (GMOY005321), was also part of the list  
347 [10]. Previous work using MIRS with other insect vectors also reported differences in female  
348 cuticles between very young and old individuals, and the model predicted 3-day old females  
349 with minimal misclassification. However, when differentiating between 5- and 7-week-olds,  
350 the misclassification between both classes increased.

351 When we used the complete spectra for training, we found that LR and SVM with a linear  
352 kernel used the region from 2500 – 1800 cm<sup>-1</sup> to predict sex and age, which does not contain  
353 any biochemical information related to insect cuticle. To ensure the algorithms learn from the  
354 biochemical differences between sexes and age groups, we restricted the inputs to specific  
355 spectral regions and limit the features the model uses. The strength of machine learning lies  
356 in finding patterns to separate classes; however, patterns can arise from confounding effects  
357 of contamination by water and CO<sub>2</sub> rather than from the structural constituents of the  
358 specimen. It is important to diagnose and assess what the model is learning to rule out any

359 bias and avoid overfitting. In spectroscopy data, variation between samples (i.e., baseline  
360 offset, variation on CO<sub>2</sub> levels during different days when measuring) was robust enough for  
361 the model to accurately classify age and sex.

362 When determining the feasibility of using different tsetse tissues for analysis, the abdomen  
363 showed inconsistent spectra compared to the head and thorax, which might be caused by the  
364 presence of blood from previous meals and incomplete desiccation. However, the  
365 information from tsetse abdomens could still be used to identify blood meal sources, as  
366 demonstrated by the application of MIRS with *Anopheles* mosquitoes [24]

367 In summary, our results provide proof-of-principle for how MIRS can detect cuticular signals  
368 linked to ageing in tsetse. Future validation of this technique using field samples is needed,  
369 where environmental cues (naturally minimised in housed insect colonies) impact ageing  
370 rates. The next step will be to test the MIRS toolbox against wild tsetse collected from  
371 endemic areas, and preferably a region currently implementing vector control strategies. The  
372 machine learning models we describe here need to be further refined using more insectary-  
373 reared flies alongside a small complementary set of field samples (age-graded when trapped)  
374 to be able to confirm the efficacy and accuracy of this technology in the field [12].

## 375 **Conclusions**

376 Our data strongly support the use of MIRS for high-accuracy age grading of both male and  
377 female *Glossina spp.* reared under insectary conditions. The protocol's robustness, minimal  
378 maintenance, cost-effectiveness, and speed make it an ideal technique for vector surveillance  
379 programmes in resource-limited settings, and implementation will strengthen ongoing  
380 control efforts to control transmission of African trypanosomiasis.

381

## 382 **Acknowledgements**

383 We are grateful to Jonathan Thornton, the dedicated technician overseeing the tsetse  
384 colony at LSTM, for his invaluable assistance in procuring tsetse flies for this work.

385

## 386 **Author contributions**

387 Conceptualization: F.B., L.R.H.

388 Data curation: M.P., K.M.S.

389 Formal analysis: M.P

390 Funding acquisition: F.B, L.R.H.

391 Investigation: M.P, I.C, K.M.S.

392 Methodology: F.B., L.R.H.

393 Project administration: F.B., L.R.H.

394 Resources: F.B., L.R.H.

395 Supervision: F.B., L.R.H

396 Visualization: M.P, K.M.S.

397 Writing – original draft: M.P.

398 Writing – review & editing: M.P, K.M.S., I.C, S.A.B., F.B, L.R.H.

399

## 400 **Funding**

401 L.R.H. was partially funded by a Wellcome Trust Institutional Strategic Support Fund (grant  
402 no. 204806/Z/16/Z) and the Biotechnology and Biological Sciences Research Council (BBSRC)  
403 Anti-VeC award (AV/PP0021/1). F.B. and M.P.B. were supported by the Academy Medical  
404 Sciences Springboard Award (ref:SBF007\100094) and by the Bill and Melinda Gates  
405 Foundation (INV-003079). K.M.S. was supported by an LSTM Director's Catalyst Fund award.

406

## 407 **Competing interests**

408 The authors declare that they have not competing interests.

## 409 **References**

- 410 1. Franco JR, Cecchi G, Paone M, Diarra A, Grout L, Kadima Ebeja A, et al. The elimination of human  
411 African trypanosomiasis: Achievements in relation to WHO road map targets for 2020. *PLoS*  
412 *Negl Trop Dis*. 2022;16: e0010047. doi:10.1371/journal.pntd.0010047
- 413 2. The disease | Programme Against African Trypanosomosis (PAAT) | Food and Agriculture  
414 Organization of the United Nations. [cited 20 Oct 2023]. Available:  
415 <https://www.fao.org/paat/the-programme/the-disease/en/>
- 416 3. Tobe SS, Langley PA. Reproductive physiology of glossina. *Annual Review of Entomology*.  
417 1978;23: 283–307. doi:10.1146/annurev.en.23.010178.001435
- 418 4. Hargrove JW. A model for the relationship between wing fray and chronological and ovarian  
419 ages in tsetse (*Glossina* spp). *Medical and Veterinary Entomology*. 2020;34: 251–263.  
420 doi:10.1111/mve.12439
- 421 5. English S, Barreaux AMG, Leyland R, Lord JS, Hargrove JW, Vale GA, et al. Investigating the  
422 unaccounted ones: insights on age-dependent reproductive loss in a viviparous fly. *Frontiers in*  
423 *Ecology and Evolution*. 2023;11. Available:  
424 <https://www.frontiersin.org/articles/10.3389/fevo.2023.1057474>
- 425 6. Pagabeleguem S, Ravel S, Dicko AH, Vreysen MJB, Parker A, Takac P, et al. Influence of  
426 temperature and relative humidity on survival and fecundity of three tsetse strains. *Parasites &*  
427 *Vectors*. 2016;9: 520. doi:10.1186/s13071-016-1805-x
- 428 7. Jackson CHN. The biology of tsetse flies. *Biol Rev Camb Philos Soc*. 1949;24: 174–199.  
429 doi:10.1111/j.1469-185x.1949.tb00574.x



- 430 8. Jackson CHN. An artificially isolated generation of tsetse flies (diptera). *Bulletin of Entomological*  
431 *Research*. 1946;37: 291–299. doi:10.1017/S0007485300022203
- 432 9. Lehane MJ, Mail TS. Determining the age of adult male and female *Glossina morsitans morsitans*  
433 using a new technique. *Ecological Entomology*. 1985;10: 219–224. doi:10.1111/j.1365-  
434 2311.1985.tb00551.x
- 435 10. Lucas ER, Darby AC, Torr SJ, Donnelly MJ. A gene expression panel for estimating age in males  
436 and females of the sleeping sickness vector *Glossina morsitans*. *PLOS Neglected Tropical*  
437 *Diseases*. 2021;15: 1–15. doi:10.1371/journal.pntd.0009797
- 438 11. González Jiménez M, Babayan SA, Khazaeli P, Doyle M, Walton F, Reedy E, et al. Prediction of  
439 mosquito species and population age structure using mid-infrared spectroscopy and  
440 supervised machine learning [version 3; peer review: 2 approved]. *Wellcome Open Research*.  
441 2019. doi:10.12688/wellcomeopenres.15201.3
- 442 12. Siria DJ, Sanou R, Mitton J, Mwanga EP, Niang A, Sare I, et al. Rapid age-grading and species  
443 identification of natural mosquitoes for malaria surveillance. *Nature Communications*.  
444 2022;13: 1–9. doi:10.1038/s41467-022-28980-8
- 445 13. Srout L, Byrd BD, Huffman SW. Classification of mosquitoes with infrared spectroscopy and  
446 partial least squares-discriminant analysis. *Appl Spectrosc*. 2020;74: 900–912.  
447 doi:10.1177/0003702820915729
- 448 14. Khoshmanesh A, Christensen D, Perez-Guaita D, Iturbe-Ormaetxe I, O’Neill SL, McNaughton D, et  
449 al. Screening of wolbachia endosymbiont infection in *aedes aegypti* mosquitoes using  
450 attenuated total reflection mid-infrared spectroscopy. *Anal Chem*. 2017;89: 5285–5293.  
451 doi:10.1021/acs.analchem.6b04827
- 452 15. Stuart BH. *Infrared spectroscopy: fundamentals and applications*. *Methods*. 2004.  
453 doi:10.1002/0470011149
- 454 16. Baker MJ, Trevisan J, Bassan P, Bhargava R, Butler HJ, Dorling KM, et al. Using Fourier transform  
455 IR spectroscopy to analyze biological materials. *Nature Protocols*. 2014;9: 1771–1791.  
456 doi:10.1038/nprot.2014.110
- 457 17. Johnson BJ, Hugo LE, Churcher TS, Ong OTW, Devine GJ. Mosquito age grading and vector-  
458 control programmes. *Trends in Parasitology*. 2020;36: 39–51. doi:10.1016/j.pt.2019.10.011
- 459 18. Langley PA, Coates TW, Carlson DA. Sex recognition pheromone in the tsetse fly *Glossina*  
460 *pallidipes* Austen. *Experientia*. 1982;38: 473–475. doi:10.1007/BF01952645
- 461 19. Babayan S, Gonzalez M. SimonAB/Gonzalez-Jimenez\_MIRS: First public release. *Zenodo*; 2019.  
462 doi:10.5281/ZENODO.2609356
- 463 20. Pedregosa F, Varoquaux G, Gramfort A, Michel V, Thirion B, Grisel O, et al. Scikit-learn: Machine  
464 learning in python. *the Journal of machine Learning research*. 2011;12: 2825–2830.
- 465 21. Eid F-E, Elmarakeby HA, Chan YA, Fornelos N, ElHefnawi M, Van Allen EM, et al. Systematic  
466 auditing is essential to debiasing machine learning in biology. *Commun Biol*. 2021;4: 1–9.  
467 doi:10.1038/s42003-021-01674-5

- 468 22. Jurenka R, Terblanche JS, Jaco Klok C, Chown SL, Krafur ES. Cuticular lipid mass and desiccation  
469 rates in *Glossina pallidipes*: interpopulation variation. *Physiological Entomology*. 2007;32: 287–  
470 293. doi:10.1111/j.1365-3032.2007.00571.x
- 471 23. Schlein Y. Age grading of tsetse flies by the cuticular growth layers in the thoracic phragma.  
472 *Annals of Tropical Medicine & Parasitology*. 1979;73: 297–298.  
473 doi:10.1080/00034983.1979.11687262
- 474 24. Mwanga EP, Mapua SA, Siria DJ, Ngowo HS, Nangacha F, Mgando J, et al. Using mid-infrared  
475 spectroscopy and supervised machine-learning to identify vertebrate blood meals in the  
476 malaria vector, *Anopheles arabiensis*. *Malaria Journal*. 2019;18: 187. doi:10.1186/s12936-019-  
477 2822-y
- 478